Potassium-promoted carbon-based iron catalyst for ammonia synthesis. Effect of Fe dispersion

Anna Jedynak [a], Dariusz Szmigiel [a], Wioletta Raróg [a], Jerzy Zieliński [b], Jerzy Pielaszek [b], Piotr Dłużewski [c], and Zbigniew Kowalczyk [a,*]

[a] Faculty of Chemistry of Warsaw University of Technology, Noakowskiego 3, 00-662 Warsaw, Poland
[b] Institute of Physical Chemistry PAS, Kasprzaka 44/52, 01-224 Warsaw, Poland
[c] Institute of Physics, Polish Academy of Science, al. Lotników 32/46, 02-668 Warsaw, Poland

Received 22 January 2002; accepted 12 March 2002

Potassium-promoted iron catalysts supported on thermally modified, partly graphitized carbon were studied in the ammonia synthesis reaction. Iron nitrate was used as a precursor of the active phase and KOH or KNO_3 were used as promoters. The kinetic studies of NH_3 synthesis were carried out in a differential reactor under 63 bar and 90 bar pressure. Hydrogen chemisorption, X-ray diffraction and transmission electron microscopy experiments were performed to determine the dispersion of iron in the specimens. All the K^+–Fe/C catalysts proved to be sensitive to ammonia, the NH_3 partial pressure dependencies of their reaction rates being close to that of the commercial magnetite catalyst (KM I, H. Topsoe). The catalytic properties of the promoted Fe particles on carbon were shown to be dependent upon the iron dispersion, *i.e.* smaller particles exhibited higher turnover frequency in NH_3 synthesis. It is suggested that either small Fe crystallites expose more highly active sites, *e.g.* C-7 (B-5) or the promotion of small crystallites by the alkali is more efficient.

KEY WORDS: ammonia synthesis; iron catalyst; carbon support; potassium promotion; iron dispersion.

1. Introduction

Ammonia synthesis from hydrogen and nitrogen still remains one of the most important processes of the chemical industry. Since Haber and Bosch, all the ammonia plants, including modern installations, operate with iron catalysts, manufactured by fusion of magnetite with small amounts of additives: K_2O, Al_2O_3, CaO. Such catalysts are stable but they display rather poor reaction rates referred to the Fe mass, due to their low dispersions (corresponding surface areas about 10–20 m^2/g). Supported iron catalysts, in spite of high Fe dispersions, have not been commercialized so far.

In the past decade, a ruthenium catalyst was introduced to industrial practice by the Kellogg Company (Kellogg Advanced Ammonia Process, KAAP) and more recently by Kellogg Brown and Root [1,2]. In contrast to promoted magnetite, the new Ru catalytic system is supported on graphitized carbon [3,4]. Recent studies performed by Shur and co-workers [5–7] demonstrate that graphitized carbon may also be applied as a support for the preparation of very active iron catalysts derived from $K_2[Fe(CO)_8]$ and doped with metallic potassium. Unfortunately, the activity was measured under a pressure of 1 bar only [5–7], which is far from the industrial reality. Since metallic potassium was introduced as the promoter, there is also doubt as to the stability of the system when operated for a long time.

Hence, the purpose of the present work was to study the catalytic behavior of the Fe/carbon systems doped with potassium ions (K^+). More specifically, the effect of iron dispersion on ammonia synthesis kinetics under elevated pressure has been investigated. Iron nitrate was used in the studies as a precursor of the active phase and potassium hydroxide (KOH) or nitrate (KNO_3) were the precursors of the K^+ ions. The dispersion of iron was determined by the hydrogen chemisorption and XRD methods, the studies being supplemented with some TEM experiments.

2. Experimental

2.1. Catalyst preparation

Two Fe/C batches of different iron contents were prepared, both supported on the same carbon material, according to the following procedure: a commercially available, amorphous active carbon (Norit RO 08) was heated (graphitized) at 1900 °C in a helium atmosphere (400 Pa) for 2 h [8]. Subsequently, the material was gasified partly in flowing CO_2 at about 840 °C up to 34% mass loss, followed by cooling in an argon stream [9]. As a consequence, a pure, graphitized carbon support of high surface area ($S_{BET} = 440\ m^2/g$) and of high

* To whom correspondence should be addressed.
E-mail: zbyko@chemix.ch.pw.edu.pl

1011-372X/02/0800-0213/0

porosity ($V_{Hg} = 1.25\,cm^3/g$) was obtained, as evidenced by the N_2 physisorption and mercury porosimetry measurements.

A precursor of the active phase ($Fe(NO_3)_3 \cdot 9H_2O$) was introduced onto the surface of the support by the multi-stage impregnation method from aqueous solutions (incipient wetness technique), followed by calcination in air at 220 °C to convert Fe nitrate into its oxide (Fe_2O_3). Then the samples were reduced in flowing hydrogen at 400 °C for 24 h and passivated with nitrogen of low oxygen concentration (0.1%). The contents of iron in the resultant materials were equal to 24 wt% (symbol Fe24/C) and 5.7 wt% (symbol Fe5.7/C), respectively. Both the Fe/C specimens were impregnated with an alcoholic solution of potassium hydroxide up to the level of K^+ : carbon = 0.23 : 1 [g : g], the former system (Fe24/C) also being impregnated with an aqueous solution of potassium nitrate (K^+ : carbon = 0.23 : 1 [g : g]).

2.2. Characterization of catalysts

The hydrogen chemisorption experiments were carried out in a glass flow setup [10,11], equipped with a gradientless reactor. The samples (500 mg) were first re-reduced in flowing hydrogen ($0.5\,cm^3/s$, 450 °C, 24 h) and flushed with helium ($0.5\,cm^3/s$, 400 °C, 0.5 h) to remove hydrogen adsorbed on the Fe surface. Then the temperature was lowered to 150 °C and helium was replaced with hydrogen ($0.5\,cm^3/s$), followed by cooling in H_2 to 0 °C. After flushing with argon ($0.5\,cm^3/s$, 0 °C, 0.25 h) to remove weakly adsorbed hydrogen, the samples were heated in an argon stream ($0.5\,cm^3/s$, 0.28 °C/s) and the amount of H_2 desorbing to an Ar stream was monitored (TPD of H_2). The dispersion of iron (fraction exposed, FE) was calculated from the integrated H_2 TPD signal, assuming the $H : Fe_s$ stoichiometry to be 1 : 1. The average size of Fe particles was calculated from the generalized equation proposed by Borodziński and Bonarowska [12].

The XRD studies were carried out in a standard Rigaku Denki diffractometer using Ni-filtered Cu K_α radiation. Samples were powdered and spread out on a porous glass. The patterns were recorded by step-by-step counting with a counting time of 10 s and a step size $2\theta = 0.05°$. The average crystallite size of iron was determined from Scherrer's equation using the full widths at half maximum of Fe reflections fitted to the analytical Pearson VII functions.

The TEM observations were performed with a JEM2000EX instrument [13] operated at an acceleration voltage of 200 kV and equipped with a double-tilted goniometer. Specimens were first ground in an agate mortar and then dispersed in *n*-butanol. Drops of the suspensions were placed on a holey carbon film supported by a copper grid. Both the XRD and TEM measurements were performed *ex situ* with samples previously tested in ammonia synthesis.

2.3. Activity measurements

The kinetic studies of NH_3 synthesis were carried out in a differential reactor supplied with a stoichiometric H_2–N_2–NH_3 mixture of controlled ammonia content (x_1)—for details see ref. [14]. Under chosen steady-state conditions of pressure, temperature, gas flow and gas composition (x_1), a small increment in the ammonia content over the sample was measured and the NH_3 synthesis rate was calculated [14], according to the mass balance for a catalyst layer. Consequently, a full ammonia partial pressure dependence of the reaction rate could be determined for each sample by changing the level of x_1 in the gas.

The kinetic experiments were performed at 400 °C and under total pressure of 63 or 90 bar—the latter value of pressure being characteristic for the modern KAAP installations [1,2] operating both with the fused iron catalyst (first bed) and Ru/carbon catalyst (the next three beds). Prior to the activity tests, the samples (of 0.1–0.4 g, depending on their activity) were *in situ* re-reduced at 450 °C for 24 h. To avoid mass and heat transfer limitations, small particles of 0.3–0.6 mm in size were tested.

3. Results and discussion

The H_2 TPD responses proved to be similar for all the K^+–F/C specimens. A symmetrical, single peak centered at about 140 °C was characteristic for each sample, contrary to what was observed for K^+–Ru/C [15], where two local maxima appeared in the signal. The H_2 chemisorption data are collected in table 1. As can be seen, the dispersion of iron particles is affected both by the metal loading and—what is unexpected—by the kind of potassium precursor: the system promoted with KNO_3 exhibits lower dispersion (FE_{H_2}) than that promoted with KOH, both derived from the same Fe24/C precursor. The reason for the difference observed is unclear. Most likely, nitrogen oxides—formed as by-products of KNO_3 decomposition during the stabilization (re-reduction) of the samples—oxidized the Fe crystallites, thus leading to the sintering effect.

The XRD patterns show (figure 1) that potassium carbonate is present in the promoted specimens, besides iron. Since the XRD experiments were performed *ex situ*, the K_2CO_3 phase might be formed during the storage of the samples in the air, which always contains small amounts of carbon dioxide. For all the specimens, the average crystallite sizes of iron estimated from line broadening (XRD column in table 1) agree very well with those calculated from the chemisorption data.

The TEM study demonstrates, in turn, that the catalysts are rather inhomogeneous as far as the dimension of the iron particles is concerned. This is exemplified in figure 2, which shows the Fe crystallite size distribution

Table 1
Dispersion of the Fe/carbon catalysts prepared

Catalyst	Chemisorption of hydrogen			XRD d_{Fe} (nm)	TEM d_{Fe} (nm)
	H_2 uptake (μmol/g_{C+Fe})	FE_{H_2} (%)	d_{Fe} (nm)		
Fe24/C	–	–	–	31	10–40
KNO_3–Fe24/C	73.5	3.4	40	48	20–100
KOH–Fe24/C	120.5	5.6	24	31	10–40
KOH–Fe5.7/C	54.2	10.6	12.5	10	–

in one of the materials (KOH–Fe24/C), the average sizes being collected in table 1. The dark-field images revealed the coarse Fe crystallites, especially in the KNO_3–Fe24/C specimen, to have regular well-faced polyhedral forms. The specific shapes (square or hexagonal, see figure 3(a)) suggest the large crystallites form rhomboid dodecahedrons (rhombidodecahedrons), that expose the Fe planes of {110} type, as shown schematically in figure 3(b).

3.1. Activity of the catalysts in NH_3 synthesis

The effect of potassium on the activity of the Fe/C catalysts has been studied first. Unfortunately, the unpromoted specimens proved to exhibit very low, hardly measurable reaction rates both at 63 and at 90 bar, when the concentration of ammonia in the gas exceeded 2–3%. Hence, to distinguish between the unpromoted samples and those promoted with the alkali, simple experiments were performed only, in which the reactor was supplied with an ammonia-free mixture ($x_1 = 0$) and the outlet concentration of NH_3 (x_2) was measured under various pressures. The results obtained for the systems containing 24% Fe are shown in figure 4(a). In both cases (Fe24/C and KOH–Fe24/C), the x_2 values increase monotonously when the pressure (p) is elevated. However, the promotional effect of potassium becomes more pronounced at higher pressures. This is clearly seen in figure 4(b), which illustrates how the ratio (n) of the integral reaction rates over KOH–Fe24/C and Fe24/C changes *versus* pressure: at $p = 90$ bar, the ratio ($n = 8$) is about four times higher than that at 4 bar ($n = 2$). The above results are in good agreement with the results reported for the fused iron catalysts [14,16], thus indicating the existence of a close similarity between the magnetite-based catalysts and iron catalysts supported on carbon.

Subsequently, the kinetic characteristics of the K^+-promoted Fe/C specimens, *i.e.* the dependencies of their reaction rates *versus* ammonia content in the gas, were determined. A fused iron catalyst (KM I, H. Topsoe) has also been tested as a reference material. Figure 5 compares the characteristics obtained for the KOH–Fe24/C sample and for KM I, under a pressure of 63 bar. Since the reaction rates were referred to iron mass (see figure 5), the comparison is not authoritative for the evaluation of the surface site activities. One may say only that both types of catalysts are kinetically similar, *i.e.* both are very sensitive to ammonia: a 20-fold drop and about a 16-fold drop in the reaction rates are observed for KOH–Fe/C and KM I, respectively, when increasing the NH_3 content from 1 to 8%.

Figure 6 presents the ammonia partial pressure dependencies of the reaction rates for all three K^+-promoted Fe/C catalysts under 90 bar pressure. Since

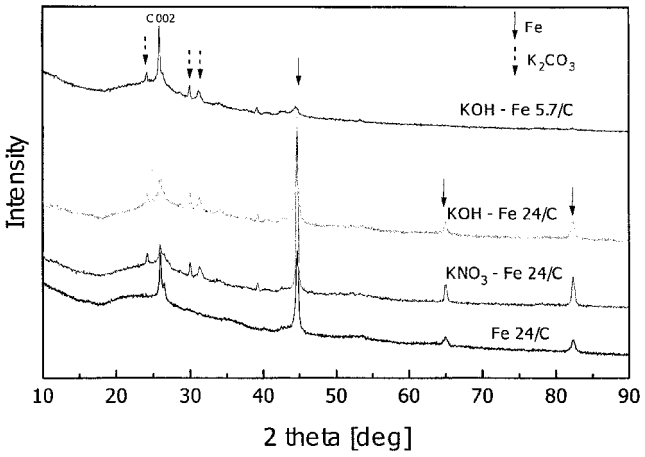

Figure 1. X-ray diffraction patterns of the carbon-based iron catalysts.

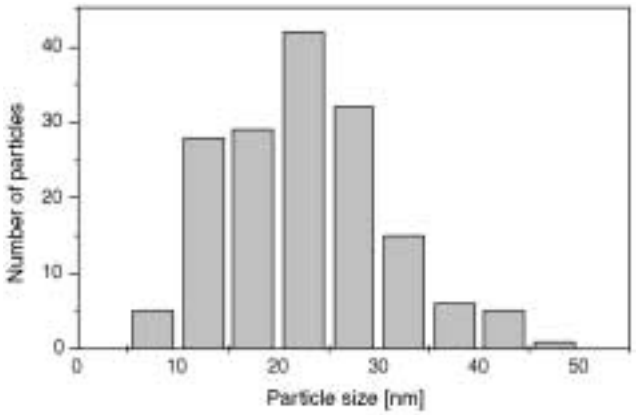

Figure 2. Distribution of the iron crystallite sizes in the KOH—Fe24/C catalyst (TEM).

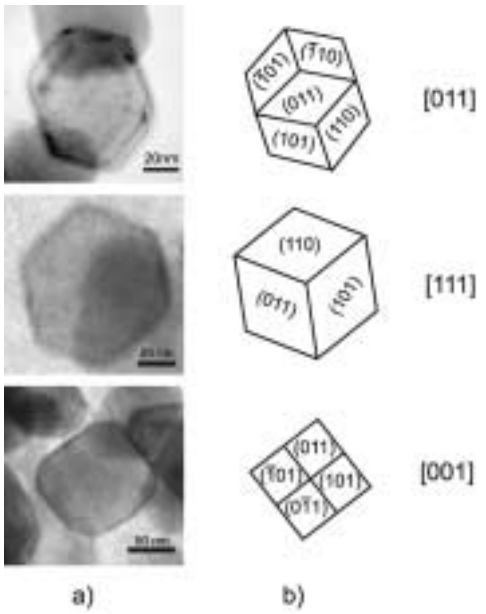

Figure 3. Well-shaped iron crystallites: (a) TEM images, and (b) corresponding projections of rhombidodecahedron with indicated {110} facets.

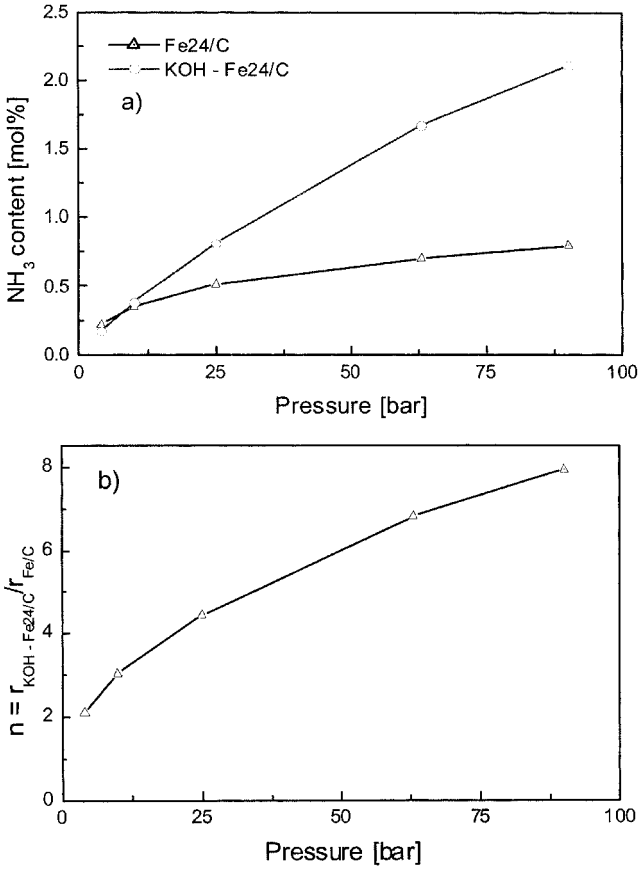

Figure 4. Effect of pressure on the activity of the Fe24/C catalysts: (a) concentration of ammonia in the outlet gas (△: Fe24/C; $T = 400\,^{\circ}C$; S.V. $= 50 \times 10^3$ l/h, ○: KOH–Fe24/C; $T = 400\,^{\circ}C$; S.V. $= 140 \times 10^3$ l/h), (b) ratio of the integral reaction rates over KOH–Fe24/C and Fe24/C ($T = 400\,^{\circ}C$).

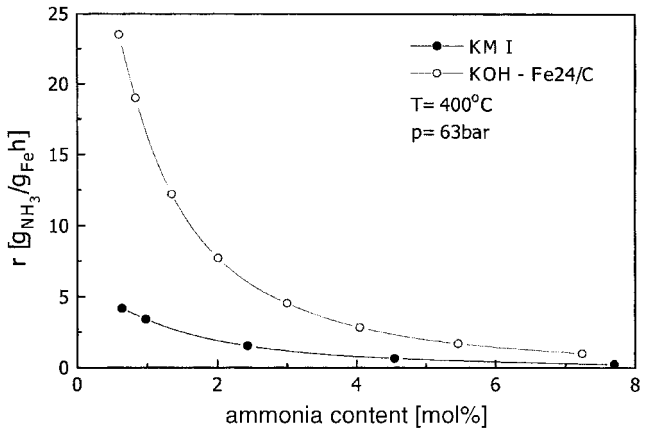

Figure 5. Ammonia partial pressure dependencies of the reaction rates over the KOH–Fe24/C catalyst and over industrial magnetite catalyst (KM I): $T = 400\,^{\circ}C$, $p = 63$ bar.

the rates of synthesis are strongly affected by ammonia, a double logarithmic scale has been used in figure 6 to distinguish between the individual traces over the whole range of NH_3 concentrations. It should be noticed that the sequence of reaction rates for the K^+–Fe/C specimens corresponds to the sequence of their dispersions listed in table 1. Since the Fe surface area is proportional to the dispersion, the above correlation seems to be obvious. However, the relationship between the turnover frequency (TOF) of NH_3 synthesis (calculated from the kinetic and H_2 chemisorption data) and the particle size (figure 7) demonstrates that the catalytic properties of iron are influenced by the Fe dispersion: the smaller the crystallites, the higher the TOF values. A reference should be given here to the early papers by Boudart and co-workers [17–19], who studied the properties of small iron particles on magnesia. Contrary to what we observed for K^+–Fe/C, they found TOF of NH_3 synthesis over Fe/MgO to be the higher, the bigger the particle size [18]. The above "discrepancy" shows clearly that the behavior of Fe particles in NH_3 synthesis depends on the kind of support, the phenomenon being

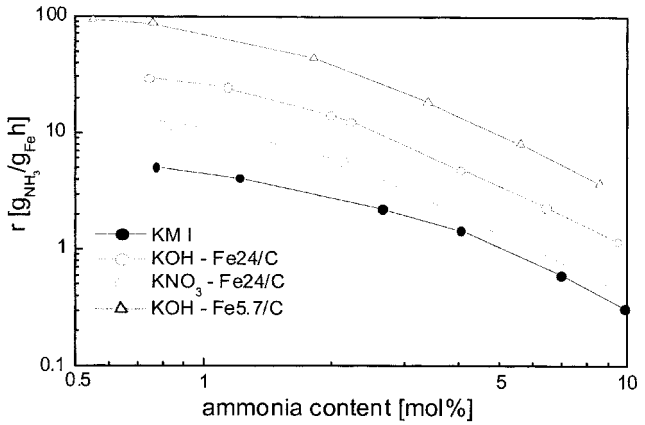

Figure 6. Ammonia partial pressure dependencies of the reaction rates over the three K^+–Fe/C catalysts under the 90 bar pressure; $T = 400\,^{\circ}C$.

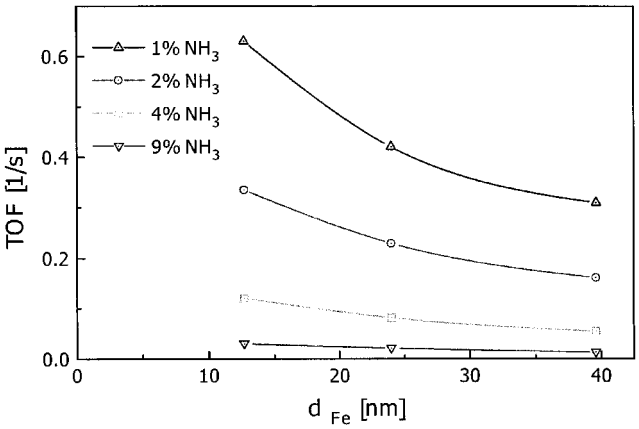

Figure 7. Turnover frequency of NH_3 synthesis over the K^+–Fe/C catalyst *versus* iron particle size for different ammonia contents in the gas: $T = 400\,^{\circ}C$; $p = 90$ bar.

well known for the unpromoted ruthenium catalysts [20–22] as well as for those promoted with the alkali [21–26].

Two possibilities should be considered when discussing the reasons for the observed decrease in TOF over K^+–Fe/C *versus* particle size:

(a) promotion by potassium is more efficient in the case of smaller Fe crystallites (effect of promotion),
(b) small crystallites expose relatively more sites of high activity, *e.g.* C-7 sites, than the larger ones (structure sensitivity effect).

The potassium promotion is commonly assumed to proceed *via* electron transfer from the alkali to the Fe surface. As a result of the $K^{\delta+}$–$Fe^{\delta-}$ electric dipole formation, the barrier for N_2 dissociation (the rate-limiting step of NH_3 synthesis) is decreased [27–30] and/or all NH_x species, including adsorbed NH_3 molecule, are destabilized [31–35]—resulting in more free sites on the active surface and thus increasing its activity [31,32]. The above concepts require potassium to be in a highly reduced state. However, the alkali metals are known to be unstable under ammonia synthesis conditions [36] and the Fe surface is thought to be covered with a composite K + O adlayer (K_xO_y groups) [28]. Oxygen partly but not totally neutralizes the promotional effect and it acts as a stabilizing agent for potassium [28,37].

Graphitized carbon is a rather untypical support that forms intercalated compounds with the alkali. Consequently, potassium is expected to exist in its zero valent state on the carbon surface. Since ionic potassium (K^+) has been used as a precursor in our studies, the overall promotional effect might originate both from K_xO_y groups that cover the Fe surface and from highly reduced potassium at contact points between the Fe crystallites and the alkali metal adsorbed onto the graphite as suggested for Ru/C [4,38] (the "hot ring promotion"). The number of K^0–Fe contact points ("hot ring") is, for obvious geometrical reason, proportional to d_{Fe}^{-2}, whereas the number of surface Fe atoms is proportional to d_{Fe}^{-1}. Hence, the higher the Fe dispersion, the larger the contribution of metallic potassium—which is, in nature, a more efficient promoter than K_xO_y—to the overall effect and the higher the turnover frequencies would result.

On the other hand, ammonia synthesis both on iron and ruthenium is known to be a structure-sensitive reaction. Somorjai and co-workers [32,39] have shown that the Fe(111) and Fe(211) planes are the most active among the low-index planes of iron. A high activity of those surfaces was attributed to the presence of the so-called C-7 sites (Fe atoms with seven nearest neighbours) [32]. In the case of ruthenium, the B-5 sites are believed to dominate the catalytic properties of the Ru surface in NH_3 synthesis. Compared with the flat terrace sites, the barrier for N_2 dissociation is smaller on the B-5 type sites [35] due to a more optimal geometry. It is suggested [35] that all ammonia synthesis catalysts expose B-5 active sites. The calculations performed by Jacobsen *et al.* [20] for ruthenium indicate that the concentration of B-5 sites increases systematically upon the Ru dispersion to reach maximum for very small particles of about 2 nm in diameter. It seems reasonable to assume that the iron particles of several nanometers are also the most advantageous, *i.e.* they expose the highest concentration of the C-7 (B-5) sites and, consequently, the highest activity referred to the Fe surface area. Hence, an increase in TOF with an iron dispersion increase, as observed for the K^+–Fe/C systems prepared (figure 7), might be attributed to the enhancement in the concentration of C-7 (B-5) sites. Further studies, with catalysts of much higher dispersion ($d_{Fe} < 10$ nm) are necessary, however, to clarify the problem.

Attention should be paid in the end to the practical aspects of the studies performed. A very active K^+–Fe/C catalyst requires iron to be finely dispersed. The activity enhancement would be double then—due to the increase in the iron surface area (for a fixed Fe loading) and due to the increase in the turnover frequencies.

4. Conclusions

1. Iron catalysts deposited on graphitized carbon and promoted with potassium ions (K^+) display a high activity in ammonia synthesis. The kinetic behavior of the K^+–Fe/C systems is similar to that of the fused iron catalyst, *i.e.* both types are very sensitive to the changes in ammonia concentration in the gas mixture ($H_2 : N_2 = 3 : 1$).
2. The catalytic properties of the Fe surfaces in K^+–Fe/C are affected by the metal dispersion: the lower the iron particle size, the higher the TOF of NH_3 synthesis. It is suggested that either the Fe surfaces of small Fe crystallites exhibit relatively more C-7 (B-5) sites—which are

suggested to be essential for the reaction rate—or the promotion of small particles by the alkali is more efficient than that of the bigger ones—due to the greater contribution of metallic potassium to the overall effect both from K^0 (“hot ring promotion”) and K_xO_y (promotion of the Fe surface).

References

[1] R.B. Strait, Nitrogen Methanol 238 (1999) 37.
[2] R.B. Strait and S.A. Knez, in: *Int. Conf. Exhibition*, Caracas, 28 February–2 March 1999.
[3] US Patent 4,163,775 (1979), British Petroleum.
[4] S.R. Tennison, in: *Catalytic Ammonia Synthesis: Fundamentals and Practice*, ed. J.R. Jennings (Plenum Press, New York, 1991), p. 303.
[5] S.M. Yunusov, E.S. Kalyuzhnaya, B.L. Moroz, S.N. Agafonova, V.A. Likholobov and V.B. Shur, J. Mol. Cat. A 165 (2001) 141.
[6] S.M. Yunusov, E.S. Kalyuzhnaya, H. Mahapatra, V.K. Puri, V.A. Likholobov and V.B. Shur, J. Mol. Cat. A 139 (1999) 219.
[7] S.M. Yunusov, E.S. Kalyuzhnaya, B.L. Moroz, S.N. Agafonova, V.A. Likholobov and V.B. Shur, Appl. Catal. A 218 (2001) 251.
[8] Z. Kowalczyk, J. Sentek, S. Jodzis, R. Diduszko, A. Presz, A. Terzyk, Z. Kucharski and J. Suwalski, Carbon 34 (1996) 404.
[9] W. Raróg, I. Lenarcik, Z. Kowalczyk, J. Sentek, M. Krukowski and J. Zieliński, Polish J. Chem. 74 (2000) 1473.
[10] J. Zieliński, J. Catal. 76 (1982) 157.
[11] Z. Kowalczyk, S. Jodzis, W. Raróg, J. Zieliński and J. Pielaszek, Appl. Catal. A 173 (1998) 153.
[12] A. Borodziński and M. Bonarowska, Langmuir 13(21) (1997) 5613.
[13] Z. Kowalczyk, J. Sentek, S. Jodzis, E. Mizera, J. Góralski, T. Paryjczak and R. Diduszko, Catal. Lett. 45 (1997) 65.
[14] Z. Kowalczyk, Catal. Lett. 37 (1996) 173.
[15] W. Raróg, Z. Kowalczyk, J. Sentek, D. Skladanowski, D. Szmigiel and J. Zieliński, Appl. Catal. A 208 (2001) 213.
[16] J. Schitze, W. Mahdi, B. Herzog and R. Schloegl, Topics Catal. 1 (1994) 195.
[17] M. Boudart, A. Delbouille, J.A. Dumesic, S. Khammoumma and H. Topsoe, J. Catal. 37 (1975) 486.
[18] J.A. Dumesic, H. Topsoe, S. Khammoumma and M. Boudart, J. Catal. 37 (1975) 503.
[19] J.A. Dumesic, H. Topsoe and M. Boudart, J. Catal. 37 (1975) 513.
[20] C.J.H. Jacobsen, P.L. Hansen, E. Torngvist, L. Jansen, D.V. Prip and J. Chorkendorff, J. Mol. Cat. A 163 (2000) 19.
[21] K. Aika, H. Hori, A. Ozaki, J. Catal. 27 (1972) 424.
[22] K. Aika, A. Ohya, A. Ozaki, Y. Inoue and I. Yasumori, J. Catal. 92 (1985) 305.
[23] K. Aika, T. Takano and S. Murata, J. Catal. 136 (1992) 126.
[24] F. Rosowski, A. Hornung, O. Hinrichsen, D. Herein, M. Muhler and G. Ertl, Appl. Catal. A 151 (1997) 443.
[25] K. Aika, T. Kawahara, S. Murata and T. Onishi, Bull. Chem. Soc. Jpn. 63 (1990) 1221.
[26] T. Hikita, K. Aika and T. Onishi, Catal. Lett. 4 (1990) 157.
[27] G. Ertl, S.B. Lee and M. Weiss, Surf. Sci. 114 (1982) 527.
[28] G. Ertl, in: *Catalytic Ammonia Synthesis: Fundamentals and Practice*, ed. J.R. Jennings (Plenum Press, New York, 1991).
[29] J.J. Mortensen, B. Hammer and J.K. Norskov, Phys. Rev. Lett. 80 (1998) 4333.
[30] J.K. Norskov, S. Holloway and N.D. Lang, Surf. Sci. 114 (1984) 65.
[31] D.R. Strongin and G.A. Somorjai, J. Catal. 109 (1988) 51.
[32] D.R. Strongin and G.A. Somorjai, in: *Catalytic Ammonia Synthesis: Fundamentals and Practice*, ed. J.R. Jennings (Plenum Press, New York, 1991).
[33] P. Stolze and J.K. Norskov, Topics Catal. 1 (1994) 253.
[34] B. Fastrup, Topics Catal. 1 (1994) 273.
[35] S. Dahl, A. Logadottir, C.J.H. Jacobsen and J.K. Norskov, Appl. Catal. A 222 (2001) 19.
[36] J.G. van Ommen, W.J. Bolnik, J. Prasad and P. Mars, J. Catal. 38 (1975) 120.
[37] H. Bludau, H. Over, T. Hertel, M. Gierer and G. Ertl, Surf. Sci. 342 (1995) 134.
[38] D. Szmigiel, H. Bielawa, M. Kurtz, O. Hinrichsen, M. Muhler, W. Raróg, S. Jodzis, Z. Kowalczyk, L. Znak and J. Zieliński, J. Catal. 205 (2002) 205.
[39] D.R. Strongin, J. Carazza, S.R. Bare and G.A. Somorjai, J. Catal. 103 (1987) 213.